CHAPTER III

RESULTS AND DISCUSSIONS

3.1 Synthesis and Characterization of Receptors 1 and 2

3.1.1 Synthesis and Characterization of Receptor 1

Synthesis of receptor **1** is shown in Scheme 3.1. The nucleophilic substitution reaction of *p-tert*-butylcalix[4]arene with 2-(4-nitrophenoxy)ethyl 4-methylbenzenesulfonate (which is prepared from 4-nitrophenol in two steps) using potassium carbonate as base gave **1a** as white solid in 67% yield. Compound **1a** reacted with ethylchloroacetate using NaH as base in THF to give the cone conformer of **1b** in 72% yield. The new signals of OCH_2CH_3 and OCH_2COOR protons were found at 4.13, 1.21 and 4.38 ppm, respectively. Subsequently, reduction of **1b** catalyzed by Raney Nickel in ethyl acetate and methanol yielded diamine **1c** quantitatively, which was immediately subjected to the reaction with ferrocene diacid chloride (prepared from ferrocene in 3 steps) in CH_2Cl_2 under nitrogen atmosphere to give the final product **1** as orange solid in 12% yield.

The cone conformation of the final product was confirmed by ^{1}H-NMR spectrum as shown in Figure 3.1. A typical AB pattern was observed for the methylene bridge ($ArCH_2Ar$) protons at 3.24 and 4.65 ppm (J = 12.8 Hz). The peaks of cyclopentadiene protons in ferrocene were appeared at 4.69 and 4.89 ppm. Moreover, the (4-amidophenoxy) ethyl groups were shown as two doublets of the aromatic proton (Ar*H*) at 6.75 and 7.21 ppm, and the ethylene protons (OCH_2CH_2O) appeared at 4.40 ppm. The NH amide protons were found at 7.37 ppm. The MALDI-TOF mass spectrum in Figure 3.2 supported the structure of compound **1** observed by an intense peak [$Fe(C_{80}H_{92}N_2O_{12})$] at m/z = 1351.45 [**1**+Na^+].

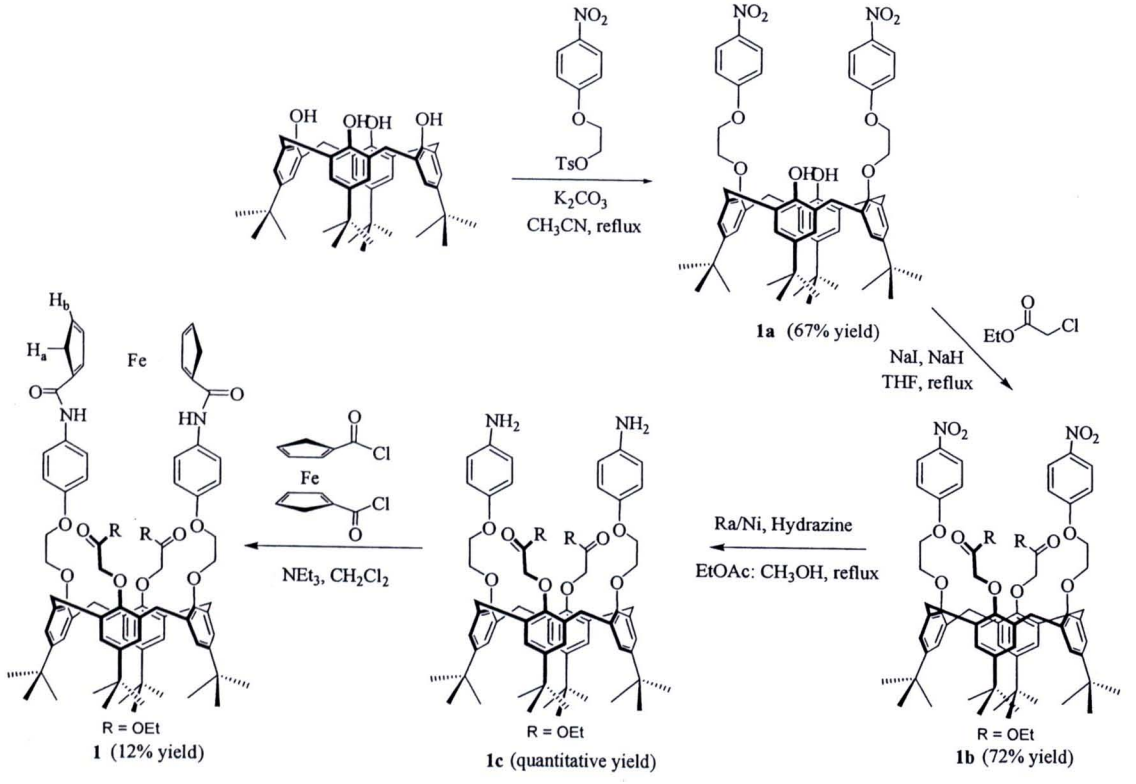

Scheme 3.1 Synthetic pathway for receptor **1**.

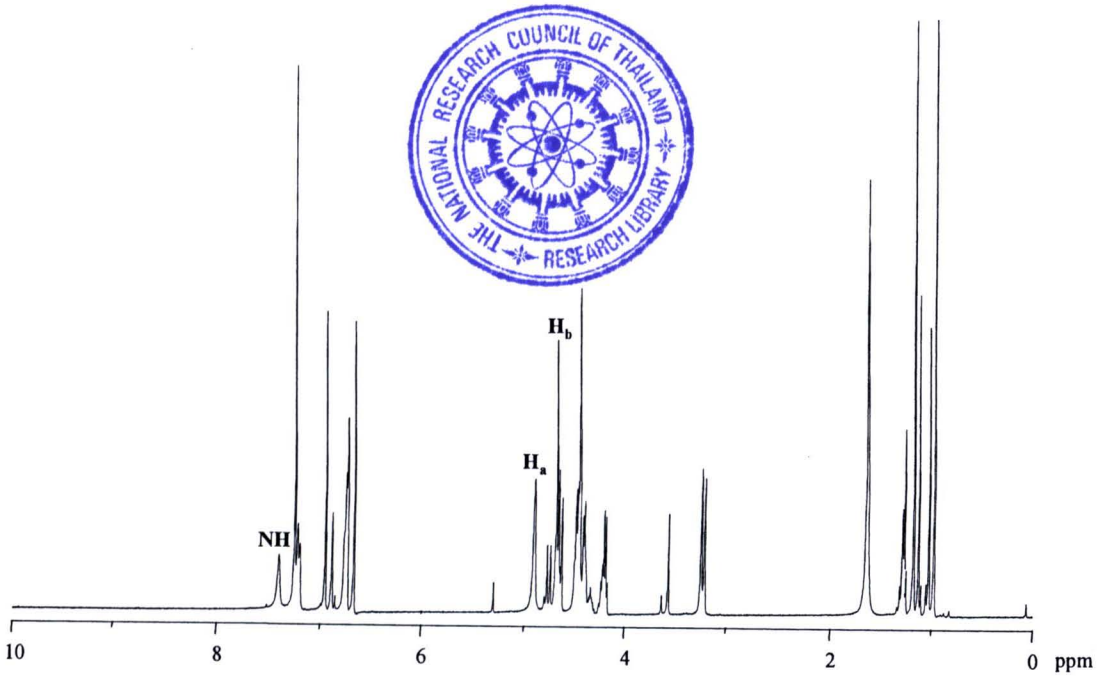

Figure 3.1 ^{1}H-NMR spectrum of receptor **1** in $CDCl_3$

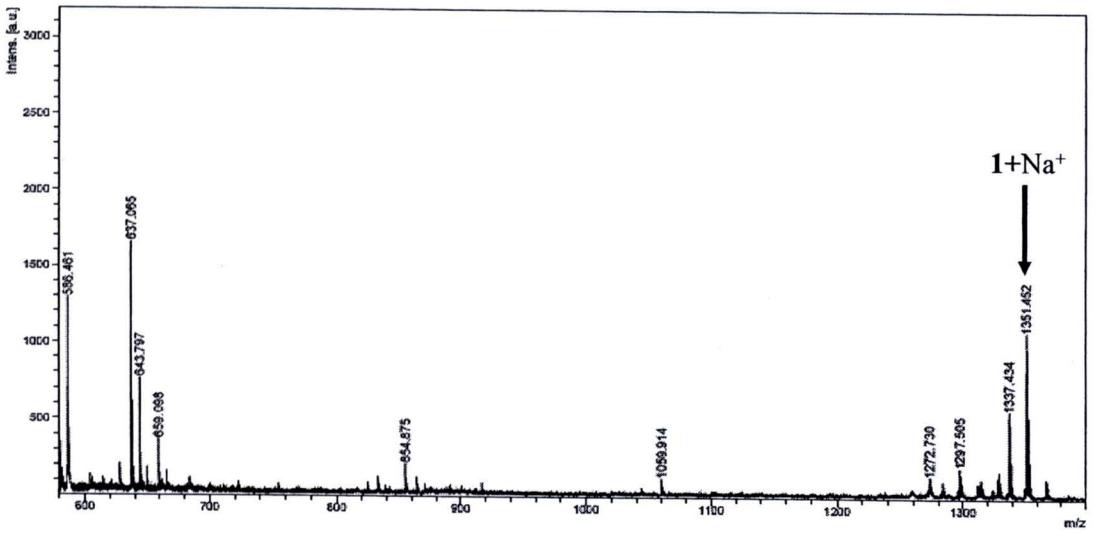

Figure 3.2 MALDI-TOF mass spectrum of receptor **1**

3.1.2 Synthesis and characterization of receptor 2

Receptor **2** can be synthesized in the similar pathway as receptor **1** which is shown in Scheme 3.2. The nucleophilic substitution reaction of *p-tert*-butylcalix[4]arene with 2-(3-nitrophenoxy)ethyl 4-methylbenzenesulfonate (prepared from 3-nitrophenol in two steps) using potassium carbonate as a base in acetonitrile gave **2a** in 62% yield. The nucleophilic substitution reaction of **2a** with ethylchloro acetate using NaH as a base in THF gave **2b** in 24% yield. The new signals of OCH_2CH_3 and OCH_2COOR protons were found at 4.10, 1.17 and 4.67 ppm, respectively. Compound **2b** was reduced by Raney Nickel in ethyl acetate and methanol gave diamine **2c** quantitatively. Finally, the compound **2c** immediately reacted with ferrocene diacid chloride in CH_2Cl_2 under nitrogen atmosphere to give product **2** as orange solid in 14% yield.

The cone conformation of the final product **2** was confirmed by ^{1}H-NMR spectrum as shown in Figure 3.3. A typical AB pattern was observed for the methylene bridge ($ArCH_2Ar$) protons at 3.14 and 4.53 ppm (J = 12.8 Hz). The peaks of cyclopentadiene protons in ferrocene were appeared at 4.47 and 4.69 ppm. Moreover, the signals in nitrobenzene group also appeared at 7.24-7.81 ppm, and the ethylene protons (OCH_2CH_2O) appeared at 4.35 and 4.38 ppm. The signal of NH amide protons reveals a large downfield shift at 8.72 ppm, suggesting that NH protons were involved in intramolecular hydrogen bonding. The MALDI-TOF mass spectrum

in Figure 3.4 confirmed the structure of compound **2** observed by an intense peak [$Fe(C_{80}H_{92}N_2O_{12})$] at m/z = 1351.187 [**2**+Na^+].

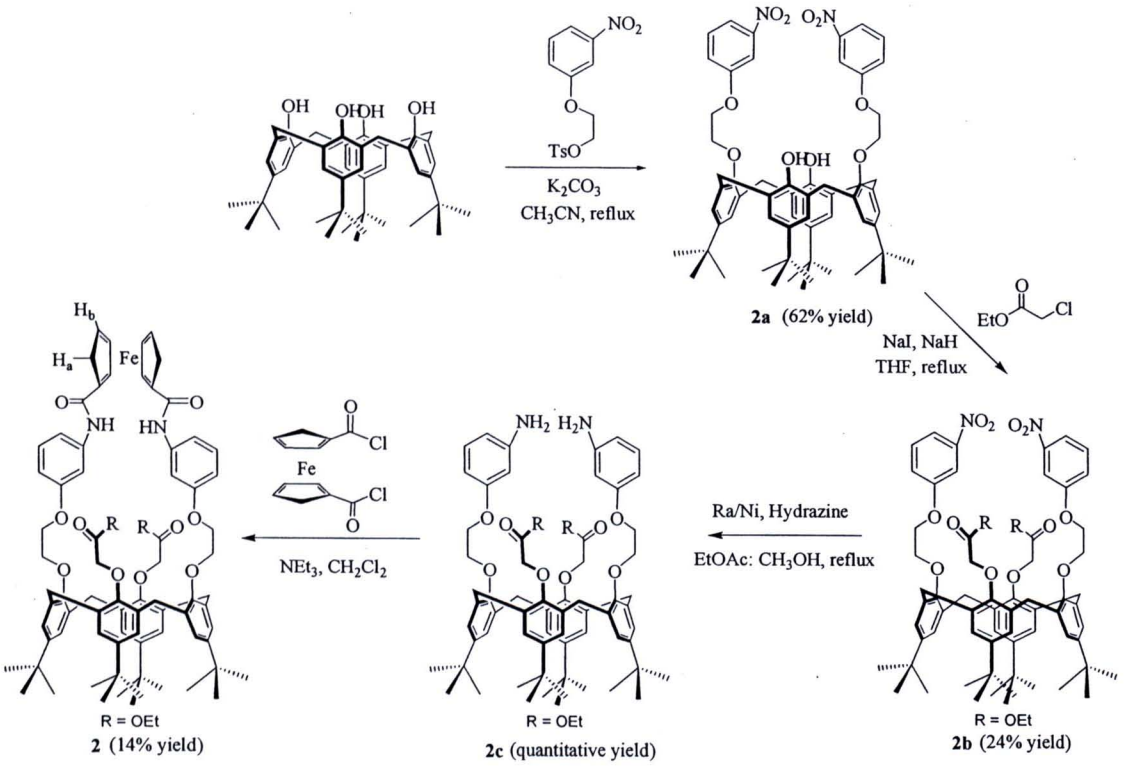

Scheme 3.2 Synthetic pathway for receptor **2**

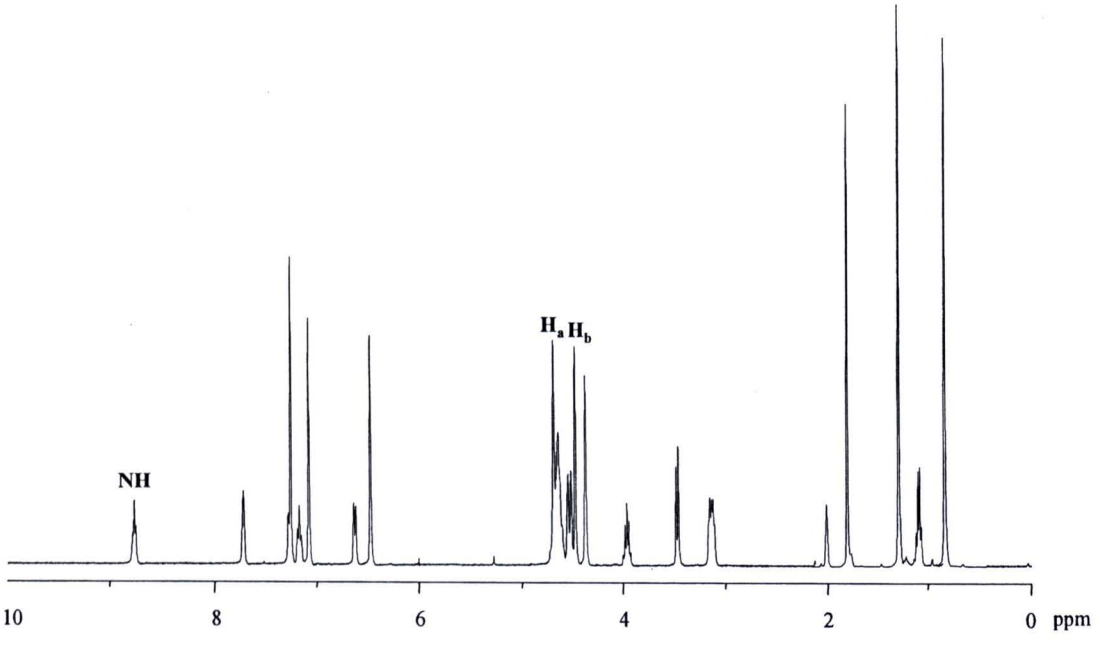

Figure 3.3 ^{1}H-NMR spectrum of receptor **2** in $CDCl_3$

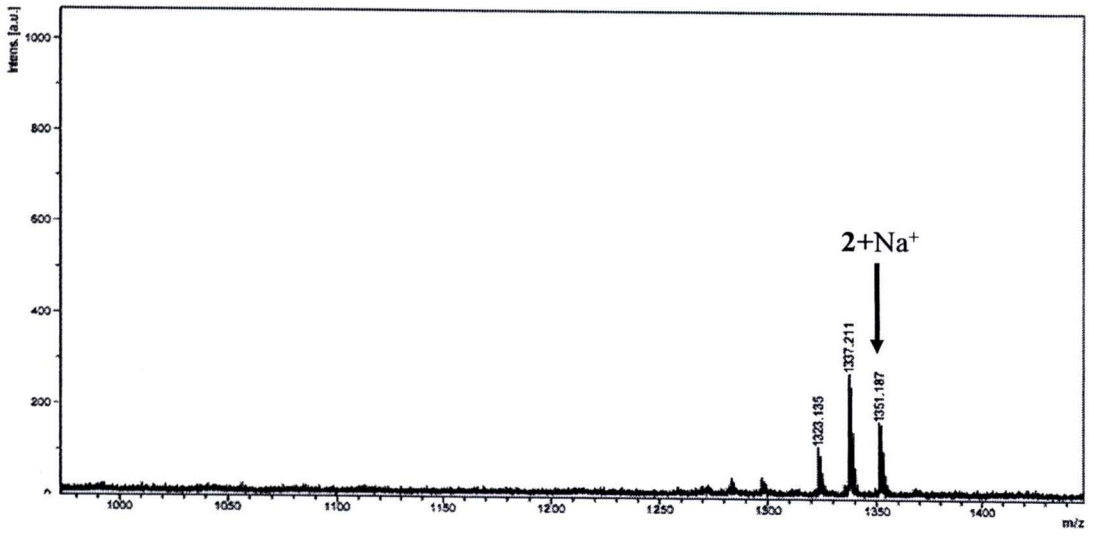

Figure 3.4 MALDI-TOF mass spectrum of receptor **2**

In this research, we expected that the sensing properties of these sensors towards anions will be controlled by co-bound metal cation and ferrocene moiety in the electrochemically oxidized form (ferrocenium cation). Electrostatic interactions of positive charge of metal cation and/or ferrocenium cation should allow the receptors to be adjusted electrostatically for binding a specific anion. Thus, the complexation and electrochemical studies of receptors **1** and **2** towards anions in the absence and presence of cations were investigated as follows.

3.2 Complexation Studies of Receptors 1 and 2 by NMR Titration.

The choice of solvent for all of the experiments was limited because all possible species in the titration experiment (receptor, ion-pair salts, cation-anion-receptor complexes) must be soluble in the selected solvent. Also, ideally the metal cation must be bound strongly so as to minimize ion-pairing outside the receptor. Taking this into account, the cation and anion coordination properties of receptors **1** and **2** were investigated by ^{1}H-NMR titration experiments in 5% CD_3CN:$CDCl_3$.

3.2.1 NMR tiration of receptors 1 and 2 towards alkali metal cations

The addition of variable amount $NaPF_6$ and KPF_6 to solutions of receptor **1** and **2** in 5% CD_3CN:$CDCl_3$ stated that under slow-exchange conditions the spectra consisted of two signals: one for complexes and another for free species. Binding constants presented in Table 3.1 were determined by direct integrations of signals

from free receptors and complex in the ^{1}H-NMR spectrum which were described by Macomber [28]. The stability constants could be determined from the variation of the intergration ratio between the complex and the free receptor at various amount of the cationic guest. When a complex formation between receptor and each cationic guest takes place, the stability constant (K) for the equilibrium is expressed as:

$$K = \frac{[C]}{([H]_0 - [C])([G]_0 - [C])}$$

$$K = \frac{n_c / [H]_0}{(1 - n_c)(R - n_c)}$$

Where $[H]_0$ represents the initial concentration of the host

$[G]_0$ represents the initial concentration of the guest

$[C]$ represents the concentration of the complex

$[C] = n_c[H]_0$

$R = [G]_0/[H]_0$

$$n_c = \frac{I_c}{I_c + I_h}$$

Where I_c represents the integration of the complex

I_h represents the integration of the host

According to the expression above, the binding constants of receptors and alkali metal cations can be calculated and several interesting results have been observed as follows. The ^{1}H-NMR spectra of receptors **1** and **2** upon addition of Na^+ and K^+ cations display some similarities. The signals of NH protons in free receptors **1** and **2** decreased while that in a complex appeared and increased. Moreover, the chemical shift of NH protons in the [**1**.Na^+], [**1**.K^+], [**2**.Na^+] and [**2**.K^+] complexes appeared downfield ($\Delta\delta$ = 0.65, 0.25, 0.73 and 0.90 ppm respectively), whereas pseudo-crown ether and CH_2 bridging methylene protons at the lower rim of receptors **1** and **2** shifted upfield as shown in Figures 3.5 and 3.6. These results showed that the alkali metal cations were encapsulated in the pseudo-crown ether cavity of receptors **1** and **2** (Figure 3.7).

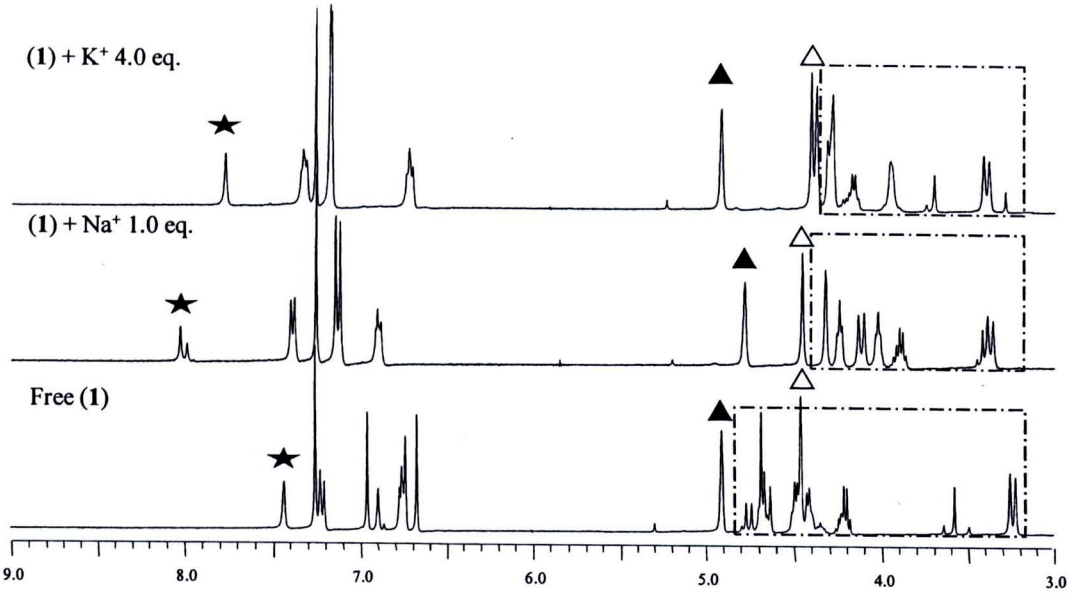

Figure 3.5 ^{1}H-NMR spectra of receptor **1** with $NaPF_6$ at 1 equivalent and KPF_6 at 4 equivalent in 5% $CD_3CN/CDCl_3$, where ★ is NH proton, ▲ and Δ are H_a and H_b protons of ferrocene and the peaks in the square refer to CH_2 protons of pseudo-crown ether moieties.

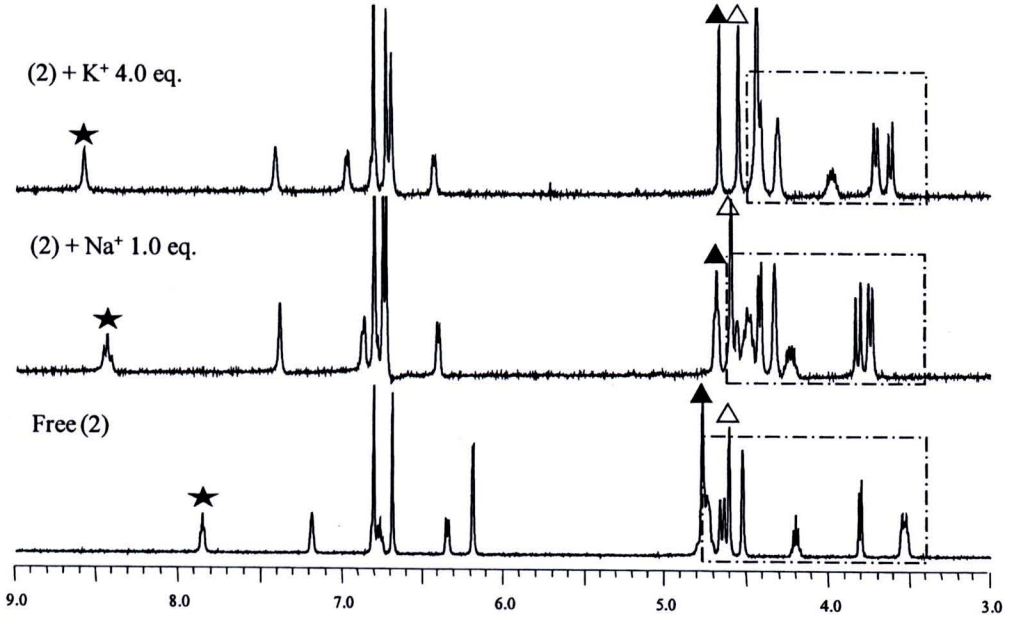

Figure 3.6 ^{1}H-NMR spectra of receptor **2** with $NaPF_6$ at 1 equivalent and KPF_6 at 4 equivalent in 5% $CD_3CN/CDCl_3$, where ★ is NH proton, ▲ and Δ are H_a and H_b protons of ferrocene and the peaks in the square refer to CH_2 protons of pseudo-crown ether moieties.

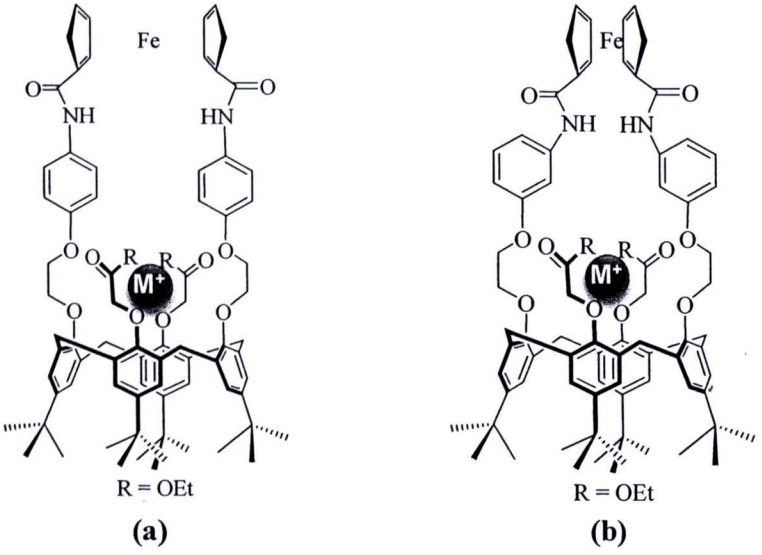

Figure 3.7 Proposed complex structures of (a) **1** and (b) **2** with alkali metal cations

In the Table 3.1, the binding constants of receptors **1** and **2** with cations show that the binding constants of both receptors **1** and **2** with Na^+ are much higher than that with K^+ which was pertinent to other crown ether or crown ether-like structure [29]. This was attributed to hard/soft acid interactions of metal cations and oxygen atom-donor of the crown ether and the bigger size of K^+ (1.36 Å) comparable to Na^+ (1.02 Å) [30]. Furthermore, the receptor/Na^+ complexes, [**1**.Na^+] and [**2**.Na^+], forms completely upon addition of 1 equivalent of Na^+ cation while the K^+ cation must add 4 equivalents to receptor **1** and 2 equivalent to receptor **2** for complete formation of receptor/K^+ complexes, [**1**.K^+] and [**2**.K^+] as shown in Figure 3.8 and 3.9. It is clear that both receptors prefer binding with Na^+ to that with K^+. Thus, Na^+ was chosen for complexing studies of receptors **1** and **2** with anionic guests in the absence and presence of Na^+.

Table 3.1 Binding constants for the Na^+ and K^+ cations complex with receptors **1** and **2** in 5% $CD_3CN/CDCl_3$

Receptor	**Binding Constant, K (M^{-1})**	
	Na^+ cation	K^+ cation
1	5670	422
2	5569	827

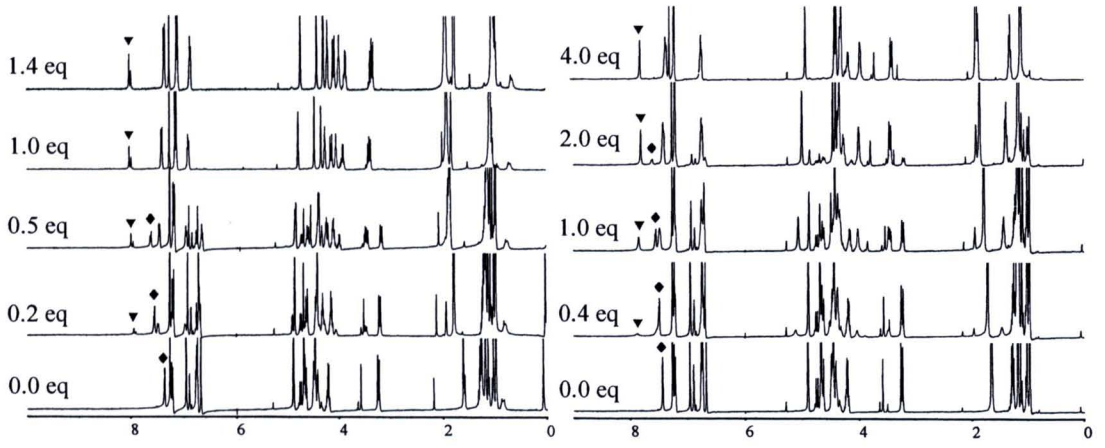

Figure 3.8 ^{1}H-NMR spectra of receptor **1** with $NaPF_6$ (left) and KPF_6 (right) in 5% $CD_3CN/CDCl_3$, where ▼ is NH protons of the [**1**.M^+] complex and ♦ is NH protons of the free receptor **1**.

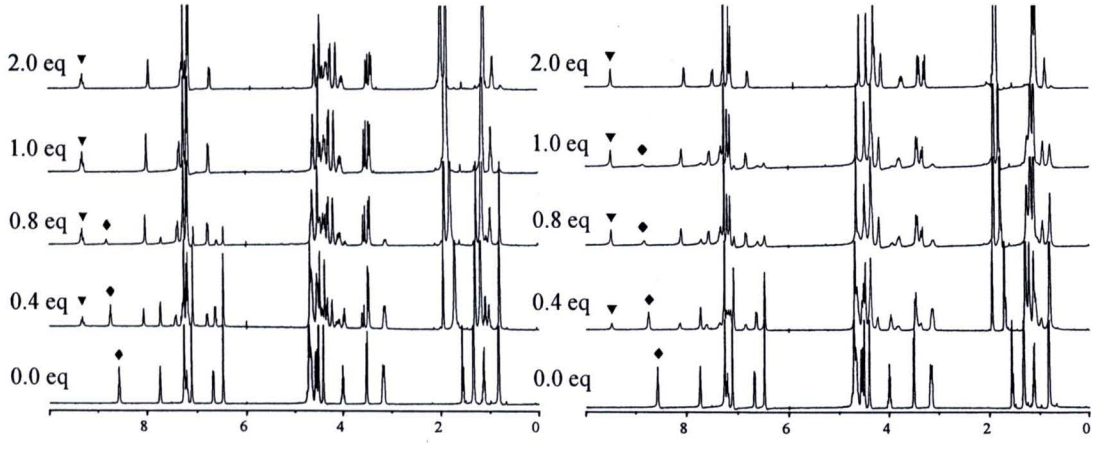

Figure 3.9 ^{1}H-NMR spectra of receptor **2** with $NaPF_6$ (left) and KPF_6 (right) in 5% $CD_3CN/CDCl_3$, where ▼ is NH protons of the [**2**.M^+] complex and ♦ is NH protons of the free receptor **2**.

3.2.2 NMR titration of receptors 1 and 2 towards anions in the absence and presence of alkali metal cation

In the same conditions, ^{1}H-NMR titration experiments were used to investigate the anion binding properties of the receptors **1** and **2** in the absence and presence of the alkali metal cations with the binding constants being obtained by analysis of the titration data with EQNMR program [31]. The binding constants for receptors **1** and **2** with anions such as benzoate, acetate, dihydrogenphosphate, chloride, bromide and iodide (added as their tetrabutylammonium salts) in the absence and presence of Na^+ cation are presented in Table 3.2.

In the absence of alkali metal cations, examination of the ^{1}H-NMR titration curves of receptors **1** and **2** upon addition of benzoate (Figure 3.10) show that the NH amide protons of both receptors continued to shift downfield indicating that the amide protons of both receptors were involved in complexing this anion in solution. The proposed structure of anion-receptor complexes are shown in Figure 3.11.

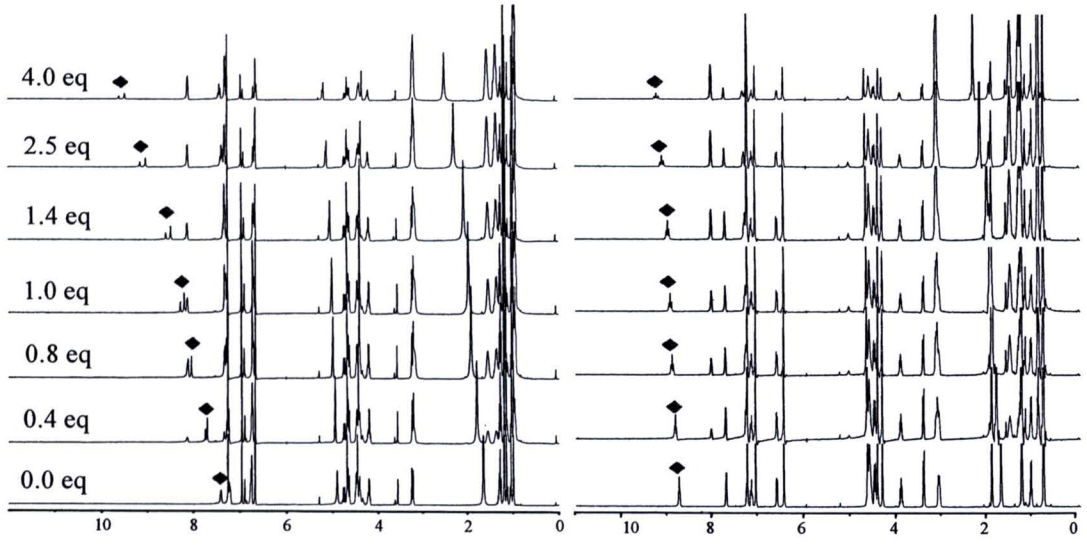

Figure 3.10 ^{1}H-NMR spectra of receptor **1** (left) and receptor **2** (right) with benzoate (added as tetrabutylammonium salt) in 5% $CD_3CN/CDCl_3$, where ♦ is NH protons upon addition of benzoate

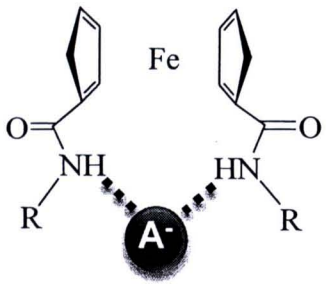

Figure 3.11 The proposed structure of amidoferrocene unit with anions

Titration isotherms obtained from these changes in the chemical shifts of the NH protons of receptors **1** and **2** were fit to the 1:1 (receptor/anion) binding model. Moreover, the titration curves of the NH proton resonance shifts of receptors **1** with anions showed that receptor **1** was able to bind anions in the following order: BzO^-, $AcO^- > H_2PO_4^- > Cl^- > Br^- > I^-$. This indicated that receptor **1** preferred forming hydrogen bonding with the Y-shaped anions (BzO^- and AcO^-) to that with the spherical (Cl^-, Br^- and I^-) or tetrahedral ($H_2PO_4^-$) anions as shown in Figure 3.12a. In the case of receptor **2**, the titration curves of receptor **2** with anions in Figure 3.12b show that receptor **2** can bind anions in the same order as receptor **1**, but the binding constants for receptor **2** with anions are very small. This may be due to intramolecular hydrogen bonding which exists between the amide groups, thus preventing anion binding. Therefore, receptor **2** can bind anions more weakly than receptor **1**.

Table 3.2 Binding constants (K) for receptors **1** and **2** with anionic guests (as tetrabutylammonium salts) in 5% CD_3CN:$CDCl_3$

	Binding Constant, K (M^{-1})					
Receptor	BzO^-	AcO^-	$H_2PO_4^-$	Cl^-	Br^-	I^-
1	66	64	32	25	-[a]	-[a]
[**1**.Na^+]	-[b]	-[b]	-[b]	-[b]	1119	886
2	25	-[a]	-[a]	-[a]	-[a]	-[a]
[**2**.Na^+]	-[b]	-[b]	-[b]	-[b]	2096	1187

[a] Values are very small and errors are more than 10%.
[b] Cannot be calculated due to ion-pair formation between bound metal cations and added anions.

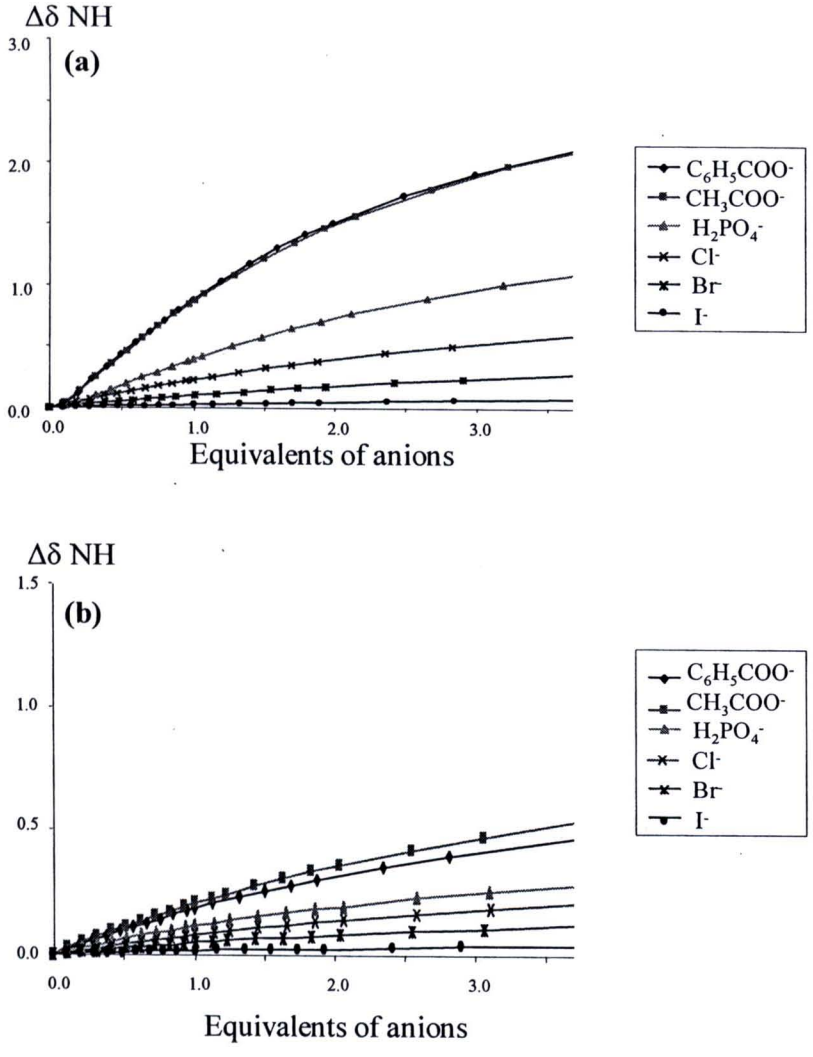

Figure 3.12 ^{1}H-NMR titration curves for NH protons in receptor **1** (a) and receptor **2** (b) upon addition of various anions.

In the presence of 1 equivalent of Na^+ cations, the ^{1}H-NMR spectra of both receptors **1** and **2** with anions were different. Upon addition of anions, the NH amide proton was monitored as shown in Figure 3.13. The binding constants can be calculated as shown in Table 3.2. The results showed that there are two types of binding occurred.

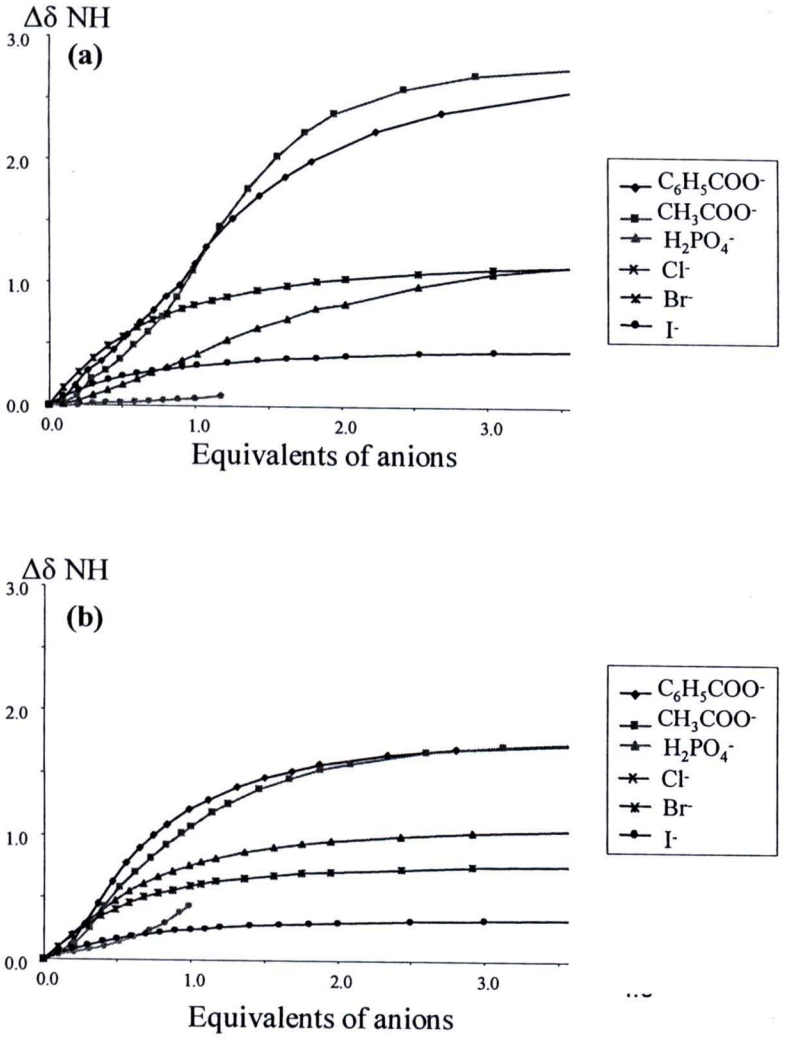

Figure 3.13 ^{1}H-NMR titration curves for NH protons in complex [**1**.Na^+] (a) and complex [**2**.Na^+] (b)

Firstly, addition of BzO^-, AcO^- and Cl^- resulted in a downfield shift of the NH proton of complexes [**1**.Na^+] and [**2**.Na^+] was observed as the same time as an appearing signal of NH proton of free receptors **1** and **2**. Moreover, the signal intensity of NH proton in both complexes decreased whereas that in both free receptors enhanced upon addition of these anions. These observations may be due to the fact that the Na^+/receptor complexes may not form completely or due to the competition of ion-pairs outside the receptors. Therefore, the 2 equivalents of Na^+ are used to prove these results in order to form the Na^+/receptor complex completely in ^{1}H-NMR titration experiments. According to the ^{1}H-NMR titration data as shown in Figure 3.14, we found that no significant change of chemical shift of NH proton was observed when 1 equivalent of the anionic guest was added. With further addition of

anions (over 1 equivalent of anion), the NH proton of the complex shifted downfield and that of free receptor appeared. These results assured us that it is due to the competition of ion-pairs outside the receptors [32, 33]. Addition of anions leads to competition among the complexation of [**1**.Na^+] and [**2**.Na^+] with anions, the formation of ion-pairs (cation and anionic guests) outside the receptors and the complexation of free receptor with anions as shown in Scheme 3.3. Therefore, the ion-pair formation between Na^+ and added anions outside the receptor has effect on the binding ability of Na^+/receptor complexes with anion.

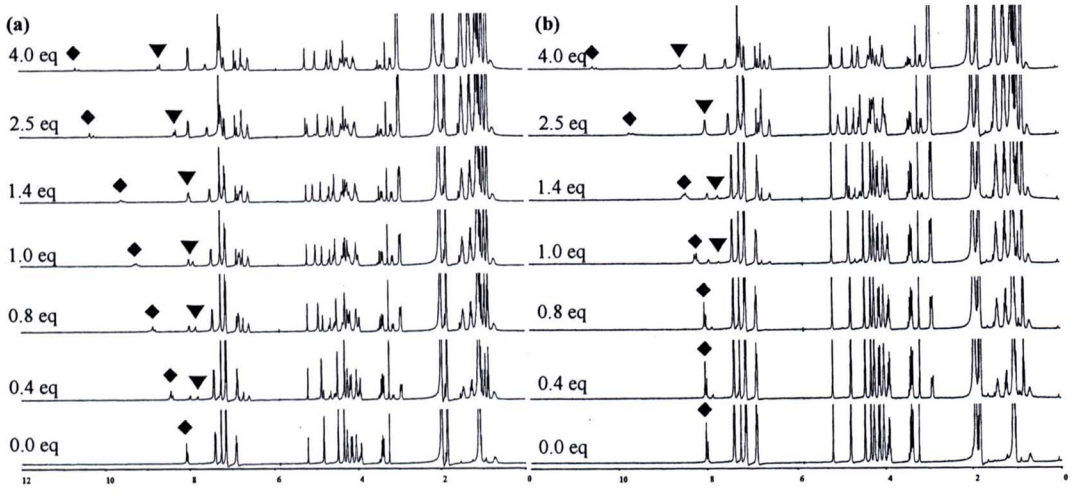

Figure 3.14 ^{1}H-NMR spectra of 1:1 mole ratio of Na^+/receptor (a) and an 2:1 mole ratio of Na^+/receptor (b) in 5% CD_3CN:$CDCl_3$ upon addition of benzoate (added as tetrabutylammonium salt), where ♦ is NH protons in Na^+/receptor complexes and ▼ is NH protons in free receptors.

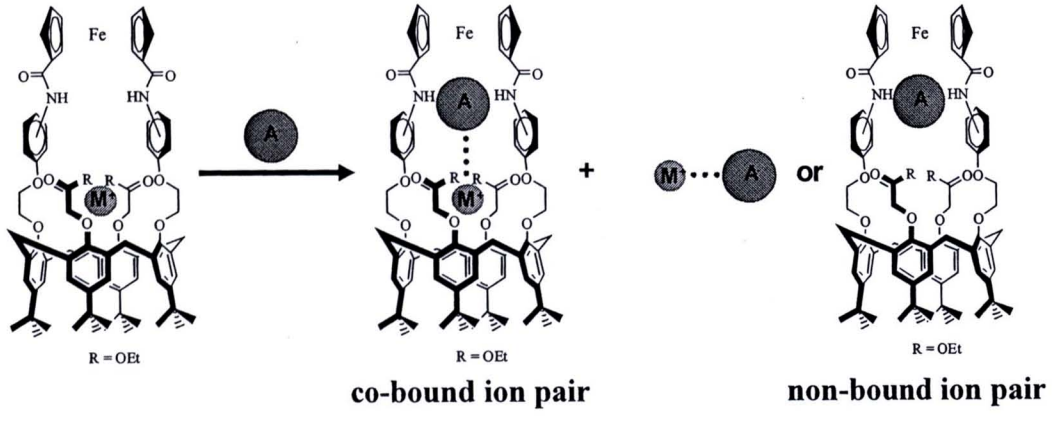

Scheme 3.3 Possible binding modes of [**1**.Na^+] and [**2**.Na^+] with anions

In the case of anion $H_2PO_4^-$, the chemical shift of NH proton in [**1**.Na^+] and [**2**.Na^+] did not change upon addition of 1 equivalent of anion $H_2PO_4^-$, whereas the signal of NH proton in both free receptors appeared and continued to shift downfield upon further addition of $H_2PO_4^-$ as shown in Figure 3.15. The results can be suggested that $H_2PO_4^-$ preferred forming the ion-pair with Na^+ in the Na^+/receptor complexes outside of the receptors to complexing with Na^+/receptor complexes. Thus, binding constants of Na^+/receptor complexes with BzO^-, AcO^-, Cl^- and $H_2PO_4^-$ cannot be calculated due to ion-pair formation between bound Na^+ and added anions.

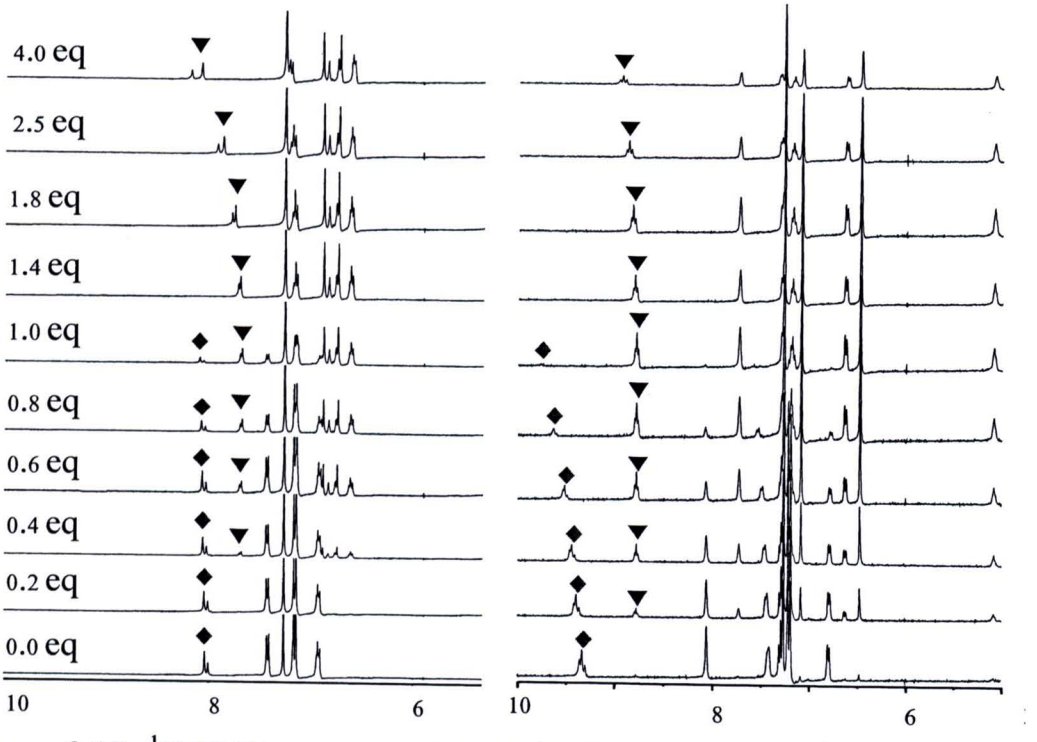

Figure 3.15 ^{1}H-NMR spectra of [**1**.Na^+] (left) and [**2**.Na^+] (right) in 5% CD_3CN:$CDCl_3$ upon addition of anion $H_2PO_4^-$, where ♦ is NH protons in complexes and ▼ is NH protons in free receptors.

Addition of Br^- and I^- resulted in a downfield shift of the NH proton of complexes [**1**.Na^+] and [**2**.Na^+] without signals of NH proton of free receptors as shown in Figure 3.16. These results are clear that addition of such anions prefer binding strongly with [**1**.Na^+] and [**2**.Na^+] to forming ion-pairs (cation and anionic guests) outside the receptors or to complexing with free receptors. Moreover, the titration curves shown in Figure 3.17 illustrated the NH amide proton of receptors **1** and **2** in the presence of Na^+ had a large downfield shift due to hydrogen bonding formation with anions directly. From Table 3.2, binding constants for both complexes

[**1**.Na^+] and [**2**.Na^+] with Br^- are highest, which indicated that the Br^- is bound much more strongly than any other anion by both receptors in the presence of Na^+. This result may be expected from size match between host cavity and Br^- anion.

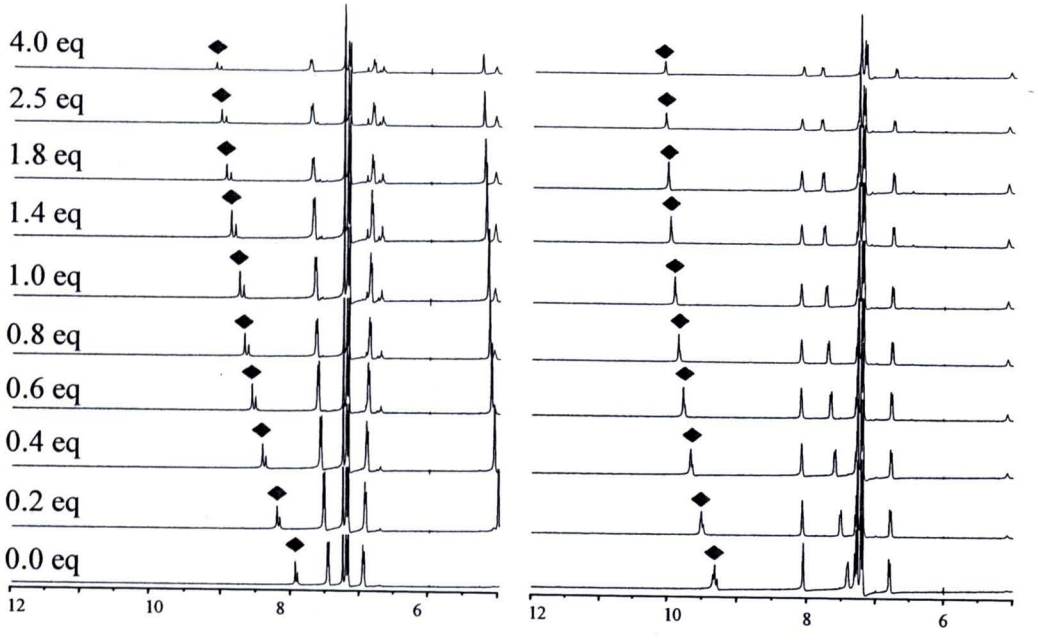

Figure 3.16 ^{1}H-NMR spectra of [**1**.Na^+] (left) and [**2**.Na^+] (right) in 5% CD_3CN:$CDCl_3$ upon addition of anion Br^- (added as tetrabutylammonium salt), where ♦ is NH protons in complexes.

Compared receptor **1** with receptor **2** in the presence of Na^+, however, binding constants for anion binding with [**2**.Na^+] are higher than those with [**1**.Na^+]. This result may be expected from size match between host cavity of receptor **2** and anions. Moreover, it should be noted that besides hydrogen bonding with NH of amidoferrocene, the weakly anion interactions of acidic Cp's CH and aromatic's CH which adjacent to amide were also observed to shift downfield.

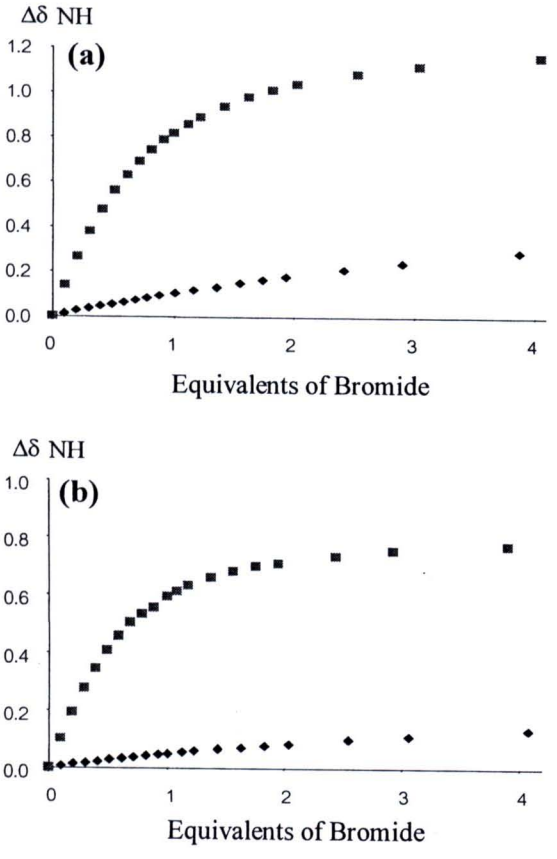

Figure 3.17 Change in NH chemical shift (Δδ) of receptor **1** (a) and receptor **2** (b) as a function of increasing tetrabutylammonium bromide, where ♦ is free receptors and ■ is receptors in the presence of Na^+.

As these results, this suggests that the Na^+ in [**1**.Na^+] and [**2**.Na^+] can enhance the binding ability of Br^- and I^- because of the electrostatic interaction of the system. Obviously, it can be seen that Na^+ "switches on" bromide bindings in both receptors **1** and **2**. Furthermore, these receptors can "switch on" iodide binding in the presence of Na^+ as well. These positive cooperative binding may be attributed to electrostatic of metal cations and anions co-bound interactions and preorganization effects of these receptors when metal cations encapsulated in the pseudo crown ether cavity.

3.3 Electrochemical Studies of Receptors 1 and 2

Synthetic receptors **1** and **2** consist of ferrocene units which are capable of electrochemical recognition for both cations and anions. Therefore, the electrochemical properties of these receptors can be studied by techniques such as cyclic voltammetry and square wave voltammetry. We have investigated the electrochemical response of the synthetic heteroditopic receptors **1** and **2** towards anions in the absence and presence of alkali metal cations by cyclic voltammetry (CV) and square wave voltammetry (SWV).

The cyclic voltammetry and the square wave techniques were performed using solutions of **1** and **2** (5×10^{-3} M) in 40% CH_3CN:CH_2Cl_2 with 0.1 M $TBAPF_6$ as supporting electrolyte and using a Pt working electrode, a Ag/Ag^+ reference electrode and a Pt coil counter electrode. All solutions were purged with N_2 before measurements. The potential was scanned in the range of 0.1 to 0.8 V at a scan rate of 100 mV/s. The cyclic voltammograms of **1** and **2** give reversibly redox couples as shown in Figure 3.18. It is obvious that the redox potential of receptor **2** is higher that that of receptor **1** suggesting that receptor **2** is harder to oxidize than receptor **1**. This may result from intramolecular hydrogen bonding between amide groups which disturbs the electrochemical properties of ferrocene unit.

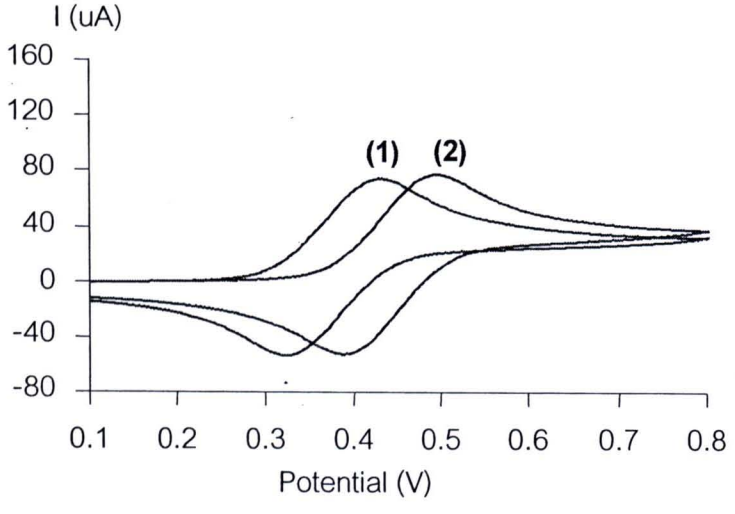

Figure 3.18 Cyclic voltammogram of receptors **1** and **2** in 40% CH_3CN:CH_2Cl_2 with 0.1 M $TBAPF_6$ at scan rate 100 mV/s.

Table 3.3 Electrochemical data (Fc/Fc^+ redox couple) of receptors **1** and **2** in 40% CH_3CN:CH_2Cl_2 with 0.1M $TBAPF_6$ at scan rate 100 mV/s.

Receptors	E_{pa} (V)	E_{pc} (V)
1	0.428	0.321
2	0.493	0.386

Studies in the area of electrochemical molecular recognition deal with bifunctional receptor molecules that contain both binding sites and redox-active sites whose electron transfer reaction are coupled to complexation. Therefore, the electrochemical properties of the ferrocene unit were perturbed upon the addition of guest molecules, either cations or anions. Such systems can be described by the scheme of one square shown in Scheme 3.4 where Fe, G and Fe-G represent the receptor, guest and complex species respectively. E^0 is the formal potential of the electron transfer reaction and K is the stability constant [34].

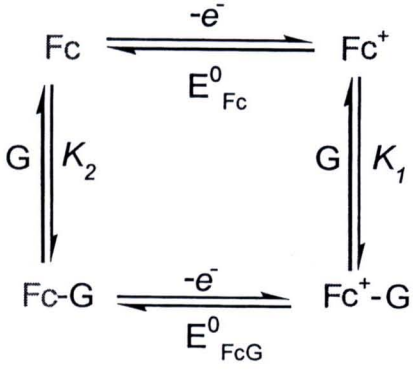

Scheme 3.4 The scheme of one square for guest binding and electron transfer.

The four reactions in Scheme 3.4 constitute a closed route, therefore the total Gibbs free energy change in this cycle is zero. To consider equilibrium to be approached via a clock-wise route starting from Fc, the statement can be mathematically expressed as in equations 3.1 and 3.2.

$$\Sigma\Delta G = \Delta G_{Fc} + \Delta G_{Fc^+} + \Delta G_{Fe^+G} + \Delta G_{FcG} = 0$$

$$nF(E - E^0_{Fc}) - RTlnK_1 + nF(E^0_{FcG} - E) + RTlnK_2 = 0 \qquad (3.1)$$

$$-nF(E^0_{FcG} - E^0_{Fc}) = RTlnK_1/K_2 \qquad (3.2)$$

From these equations, the stability constants K_1 and K_2 of a complex in different oxidation states can be observed from experimentally measurable with redox potentials E^0_{Fe} and E^0_{FeG}. The quotient K_1/K_2 is a theoretically useful parameter because it allows not only the calculation of K_1 if K_2 is known, but also the evaluation of the effect of electron transfer on the complexation. It has been termed the binding enhancement factor (BEF) [35]. However, guest binding by a redox active molecular receptors is not always enhanced upon electron transfer. Beer and co-workers have proposed that a better description for this quantity would be the reaction coupling efficiency (RCE) [36].

We expected that these sensors can be able to respond to the binding of the guest with a significant change in their redox potential that is shown in Scheme 3.5. Addition of cations causes anodic shift of the Fc/Fc^+ redox-process or a shift in the redox potential to the more positive, because the positively charged cation-receptor complex will be harder to oxidize than the neutral receptor alone [37]. Addition of anions causes cathodic shift in their redox-process because complexing to anion is easier to oxidize than free redox-active receptor [38]. Addition of anion in the presence of cation displays a large cathodic shift in Fc/Fc^+ redox process because of the strong electrostatic interactions between doubly positively charge of receptor $[Fc^+.M^+]$ in oxidized form and negatively charge of anion.

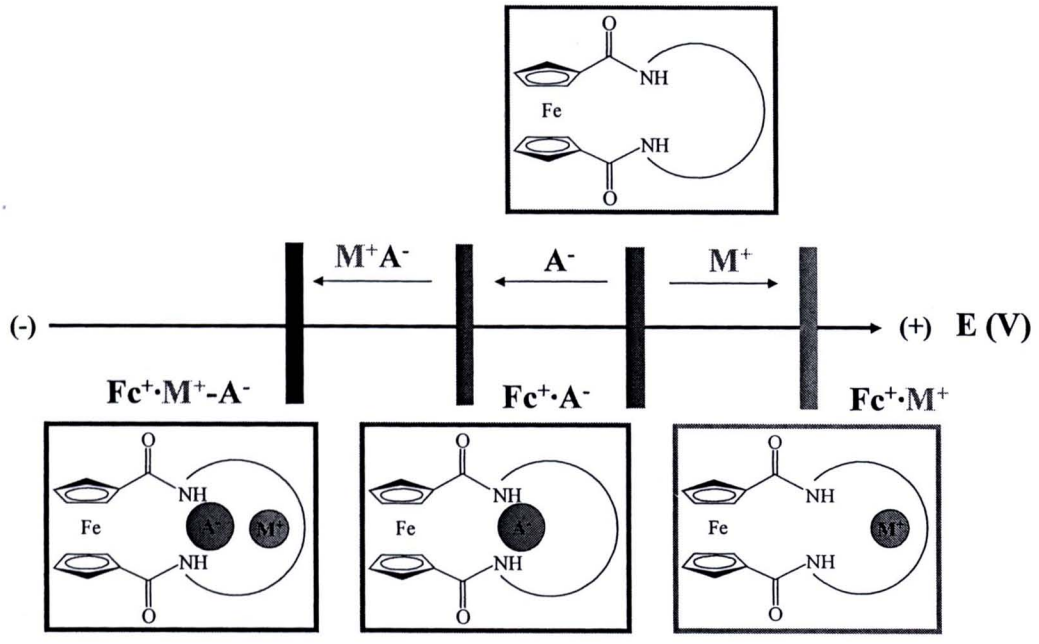

Scheme 3.5 Proposed the changed redox potential of ferrocene moiety upon cationic and/or anionic guests binding

3.3.1 Electrochemical studies of receptors 1 and 2 towards cations

According to Figure 3.19 and Figure 3.20, monitoring perturbations in the electrochemical behavior of redox-active receptor species upon addition of cations resulted in the anodic shift of the Fc/Fc^+ redox-process being observed as the positively charged cation-receptor complex will be harder to oxidize than the neutral one as be described before. Moreover, it is also implied that during the oxidation process the electrostatic repulsion between the complexed cation and the oxidized ferrocene unit (ferrocenium ion) are generated. Therefore, the oxidation of destabilized ferrocenium form of metal complex takes place at more positive potentials than the oxidation of the free receptor.

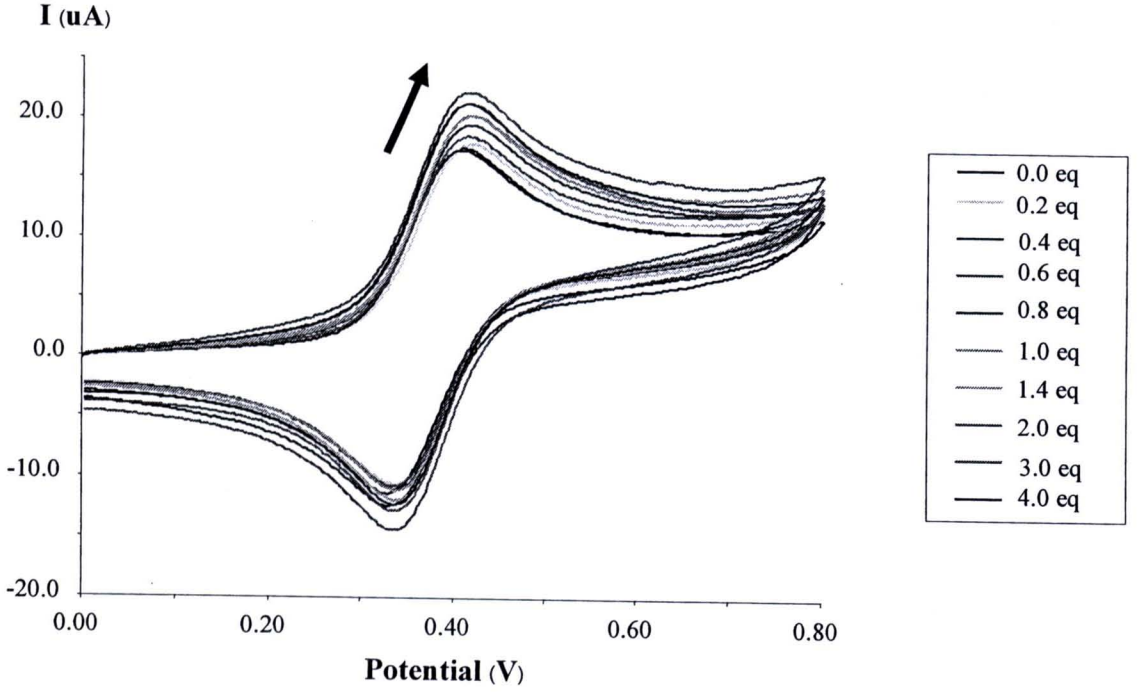

Figure 3.19 Cyclic voltammograms titration of receptor **1** with $NaClO_4$ in 40% CH_3CN:CH_2Cl_2 with 0.1M $TBAPF_6$ at scan rate 100 mV/s

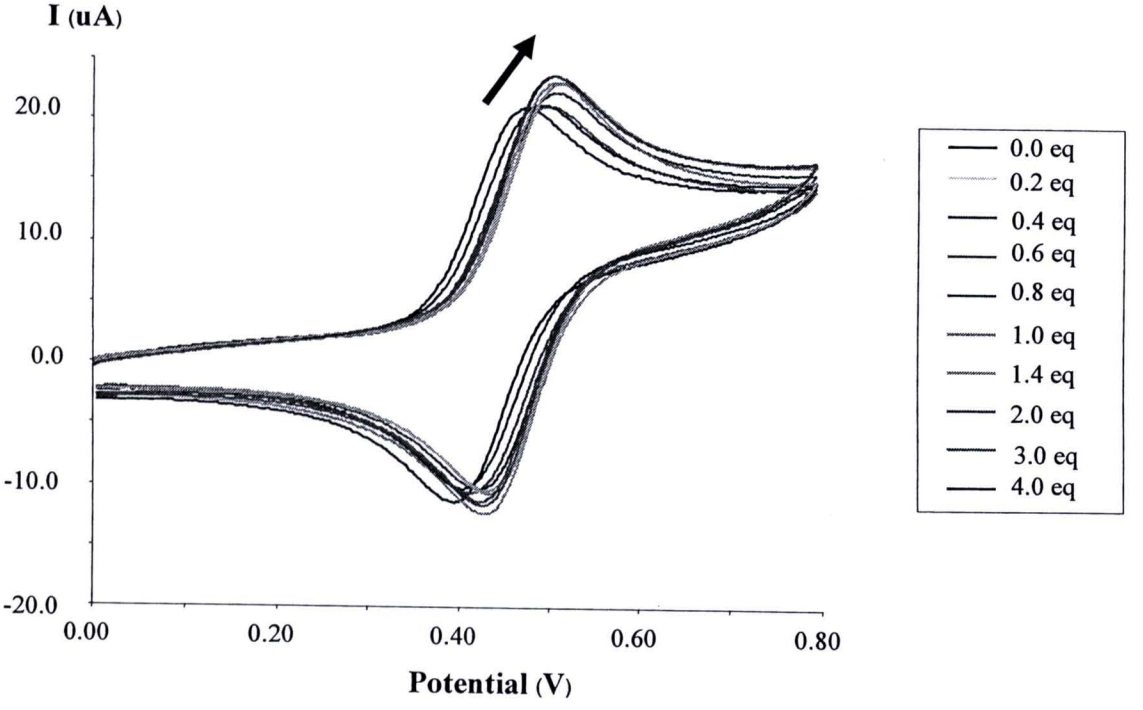

Figure 3.20 Cyclic voltammograms titration of receptor **2** with $NaClO_4$ in 40% CH_3CN:CH_2Cl_2 with 0.1M $TBAPF_6$ at scan rate 100 mV/s

The quantitative values of the reaction coupling efficiency (K_1/K_2), or RCEs, for receptors **1** and **2** can be calculated from the equation (3.2). The difference of formal redox potentials ($E^0_{FcG} - E^0_{Fc}$) or ΔE is the shift in the reduction potential caused by the complexation with metal cations.

Table 3.4 Cyclic voltammetric data and calculated binding constants (K_1) of the complexes **1** and **2** with Na^+ and K^+ in 40% CH_3CN:CH_2Cl_2 with 0.1M $TBAPF_6$ at scan rate 100 mV/s

	Receptor 1		**Receptor 2**	
	[**1**.Na^+]	[**1**.K^+]	[**2**.Na^+]	[**2**.K^+]
ΔE[a]	7	-[d]	42	-[d]
K_2[b]	5670	422	5569	827
K_1	4317	-[e]	1085	-[e]
RCE[c]	0.76	-[e]	0.19	-[e]

[a] ΔE is defined as E_{pa}(complex) – E_{pa}(receptor).

[b] Calculated from NMR titration experiments.

[c] Reaction Coupling Efficiency (K_1/K_2).

[d] Values are very small. [e] Could not be calculated.

According to Table 3.4, ΔE of receptors **1** and **2** upon addition of cations increases in the order $Na^+ > K^+$ as expected from the increasing charge-to-size ratios of those cations [39]. Compared complexes [**1**.Na^+] with [**2**.Na^+], the ΔE value of receptor **2** with Na^+ is much higher than that of receptor **1** with Na^+. This is probably due to the distance between the iron atom and the bound cations in the receptor **2** is more closer than that in the receptor **1** giving in the strong electrostatic repulsion between ferrocenium ion and a bound cation.

3.3.2 Electrochemical studies of receptors 1 and 2 towards anions in the absence and presence of alkali metal cations.

In the absence of alkali metal cation, the interactions of receptors **1** and **2** with tetrabutylammonium salts of benzoate, acetate, bromide and chloride were investigated electrochemically. Unfortunately, the redox process corresponding to iodide oxidation overlabs with the ferrocene redox wave, so the electrochemical behavior of receptors with iodide anion could not be monitored. Upon addition of anions, electrochemical receptors for anions show progressive cathodic shifts in their redox-process when complexed to an anion as they are either easier to oxidize or harder to reduce than the free redox-active receptor as shown in Scheme 3.5. The feature of cyclic voltammograms and square wave voltammograms of receptors **1** with acetate and chloride are shown in Figure 3.21 and Figure 3.22. Normally, the results obtain on the stepwise addition of anionic guest species to the receptors solutions revealed two different electrochemical behaviors: shift behavior and two wave behavior [40]. Titration of both receptors **1** and **2** with acetate display two wave behavior, the progressive appearance of a new wave at a less positive potential and a progressive disappearance of the initial wave. In contrast, cyclic voltammograms behaviors of receptors **1** and **2** with chloride and bromide show cathodic shift in Fc/Fc^+ redox potential (shift behavior) as well as decrease in current, a behavior attributed to the formation of the receptor-anion complex with a lower diffusion coefficient. Moreover, the complexes of both receptors with anions show irreversible electrochemical systems.

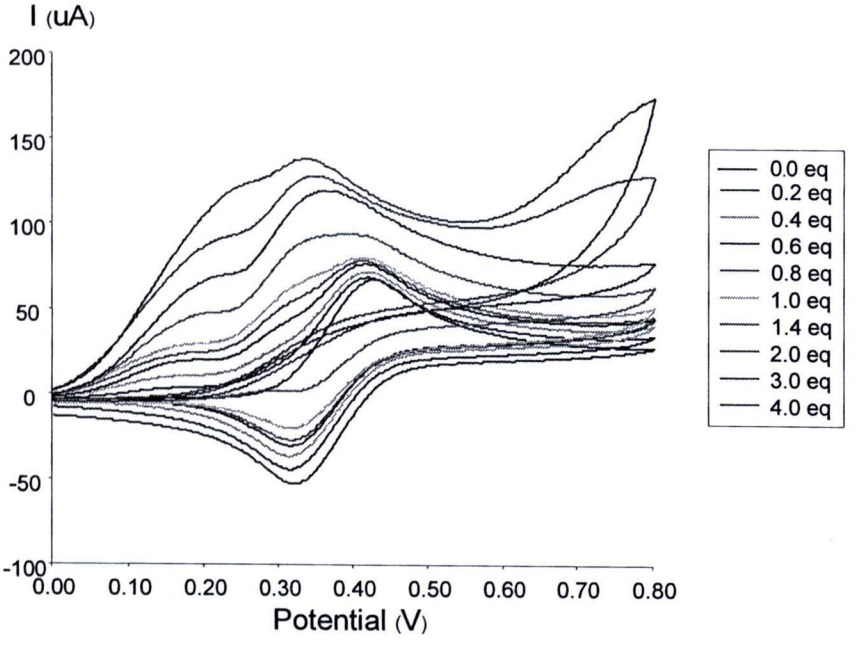

(a) Cyclic voltammogram titration

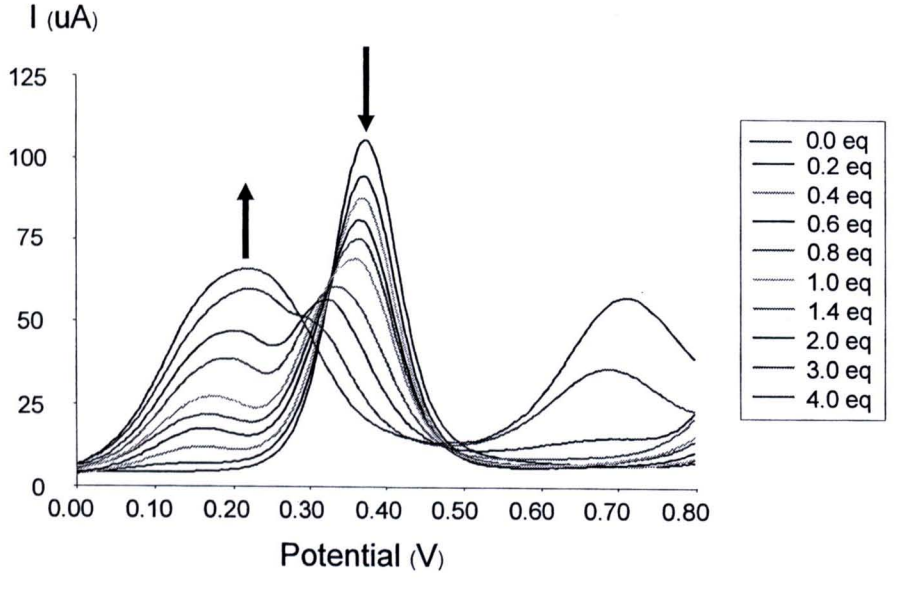

(b) Square wave voltammogram titration

Figure 3.21 Titration of receptors **1** with acetate anion in 40% CH_3CN:CH_2Cl_2 with 0.1M $TBAPF_6$ at scan rate 100 mV/s

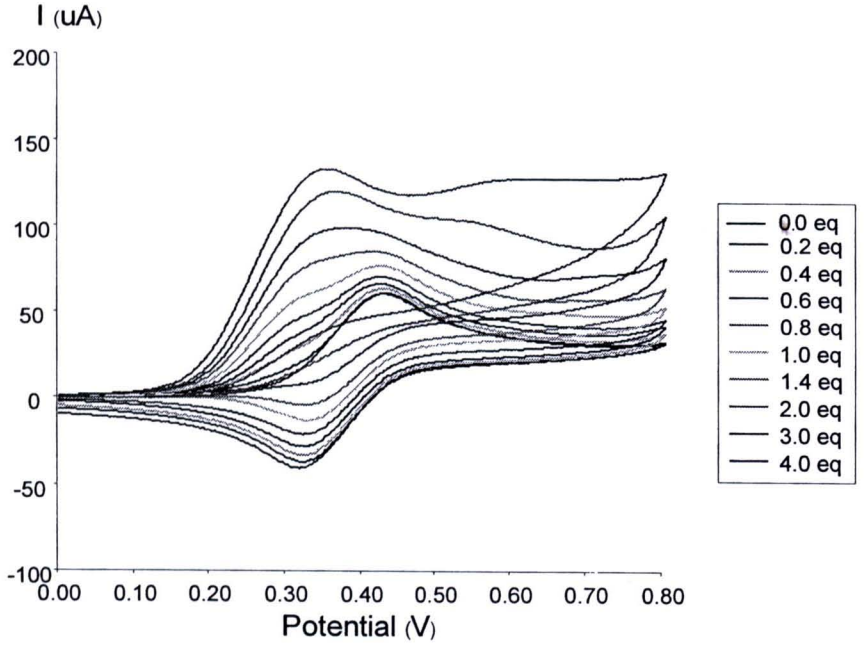

(a) Cyclic voltammogram titration

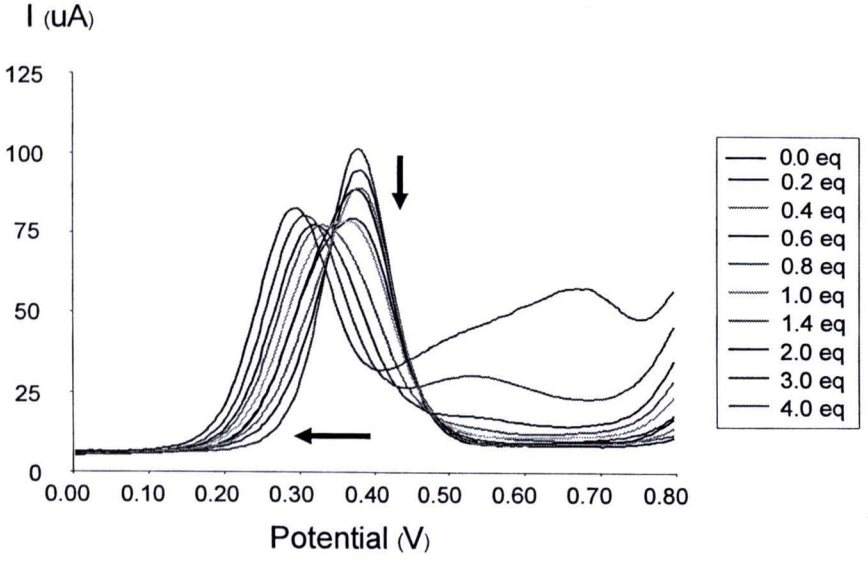

(b) Square wave voltammogram titration

Figure 3.22 Titration of receptors **1** with chloride anion in 40% CH_3CN:CH_2Cl_2 with 0.1M $TBAPF_6$ at scan rate 100 mV/s

In this case, we can expect that K_1 would be higher than K_2 rising from electrostatic interactions between anions and ferrocenium cation complementarily with the strong hydrogen bonding through the NH amide group. In other words, since anion binds more strongly to the cationic ferrocenium form of the receptor, the neutral receptor becomes easier to oxidize and the potential of the Fc/Fc^+ system shifts negatively, depended on the reinforced interactions through oxidation of the receptors. Therefore, the binding enhancement factor (BEF) in anion binding can be directly related to the redox shift induced by addition of anions.

In the presence of alkali metal cation, the addition of increasing amounts of anioinic guests to the receptors **1** and **2** cause both two-wave behavior and shift behavior in CV waves. In the systems of $[\mathbf{2}.Na^+]/AcO^-$ and $[\mathbf{2}.Na^+]/Cl^-$ display the two-wave behavior in which the progressive appearance of a new wave at the less potential and a progressive disappearance of the initial wave were observed as shown in Figure 3.23. The results obtain the new wave corresponding to the double positively charged complexed receptor, $[R^+.M^+]/A^-$ together with the initial wave corresponding to the uncomplexed receptor, $[R^+.M^+]$. Their new wave positions with respect to the uncomplexed receptors reflect a more favorable oxidation process for the ferrocene unit in the complexed spicies during guest binding. The observed negative shift is due to a reinforcement of the interaction between anions and oxidized doubly positively charged $[R^+.M^+]$ as well as stabilization of ferrocenium moieties with anions. Moreover, the complexed receptors show irreversible electrochemical behavior.

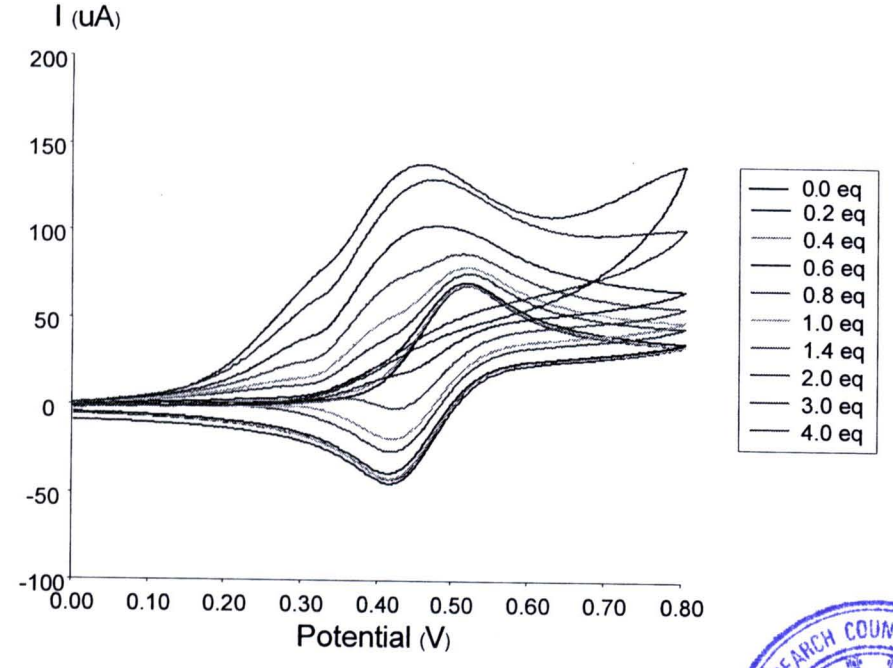

(a) Cyclic voltammograms titration

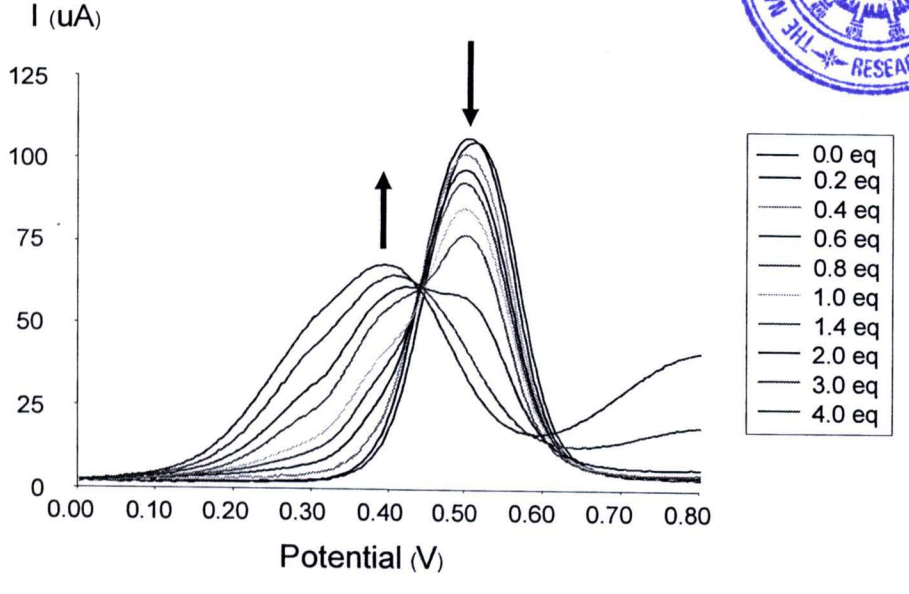

(b) Square wave voltammograms titration

Figure 3.23 Titration of [**2**.Na^+] complex with acetate anion in 40% CH_3CN:CH_2Cl_2 with 0.1M $TBAPF_6$ at scan rate 100 mV/s

In contrast, the shift behaviors were found in the system of [**1**.Na^+]/AcO^- and [**1**.Na^+]/Cl^- as shown in Figure 3.24. The cyclic voltammograms of these systems display cathodic shift in Fc/Fc^+ redox coupling than their free forms. Unfortunately, there are some precipitation problems in the systems of [**1**.Na^+]/BzO^- , [**1**.Na^+]/Br^-, [**2**.Na^+]/BzO^- and [**2**.Na^+]/Br^-.

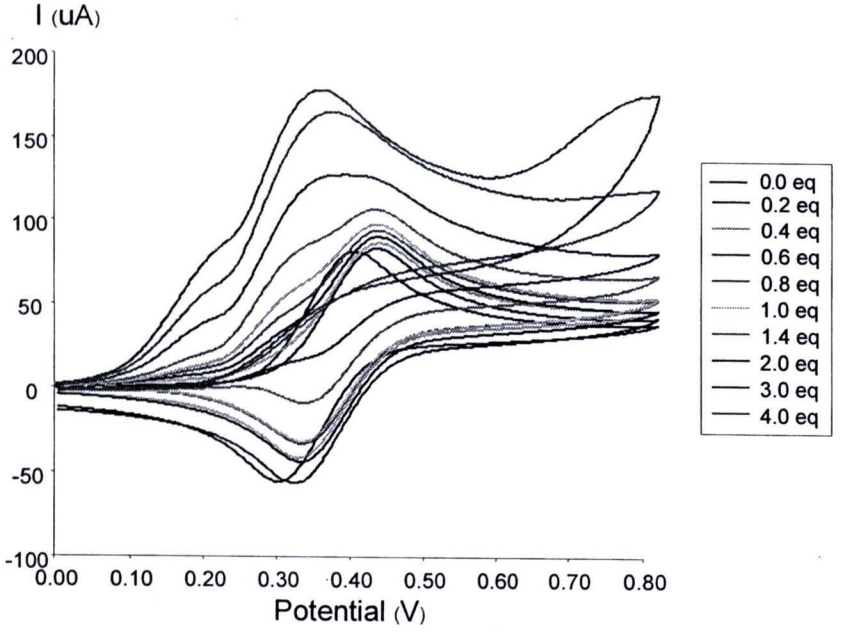

(a) Cyclic voltammograms titration

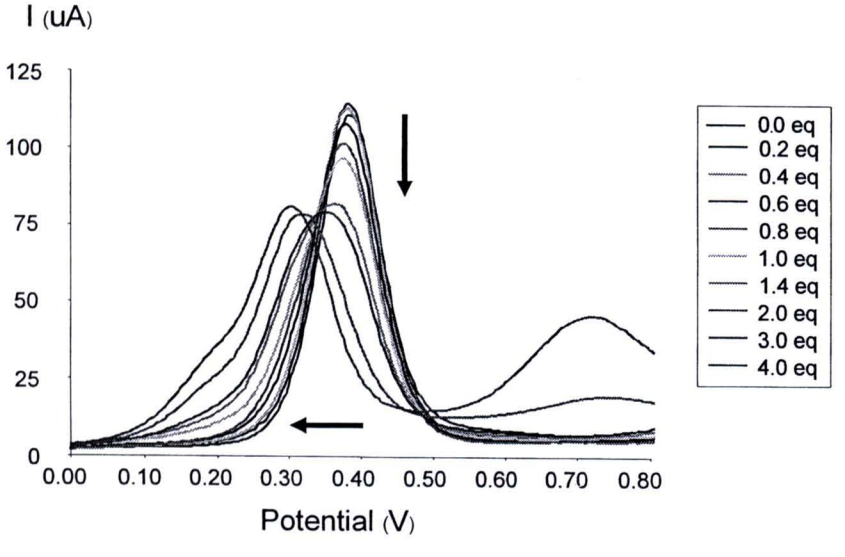

(b) Square wave voltammograms titration

Figure 3.24 Titration of [**1**.Na^+] complex with acetate anion in 40% CH_3CN:CH_2Cl_2 with 0.1M $TBAPF_6$ at scan rate 100 mV/s

In this system, K_1 value is expected that it will be higher than its neutral K_2 due to the strong electrostatic interaction between doubly positively charge of complex [Fc^+.M^+] and negatively charge of anion complementarily with the formation of [Fc^+.M^+]/A^-. However, according to the electrochemical recognition data (ΔE) as shown in Table 3.5, we found that no significant increase of ΔE for receptor **1** towards acetate and chloride were observed when the Na^+ cation was added. Moreover, the

difference between the ΔE of the free receptor **1** and the co-bound complex [**1**.Na^+] is small (the ΔE = 7 mV) as shown in Table 3.4. These observations may be due to the long distance between cation binding sites and ferrocene moiety of receptor **1**. Therefore, in the anion binding of receptor **1**, the absence and presence of cation have little effect of the electrochemical change of ferrocene moiety in the receptor **1**. In the case of receptor **2**, the magnitudes in changes of the redox potential towards anions, especially with acetate and chloride are higher than their free forms in the presence of sodium. Therefore, sensing properties of receptor **2** will be controlled by both co-bound metal cation and ferrocene moiety in the electrochemically oxidized form.

Table 3.5 Electrochemical recognition data (ΔE)[a] for receptors 1 and **2** towards anions in 40% CH_3CN:CH_2Cl_2 with 0.1M $TBAPF_6$ at scan rate 100 mV/s

Receptor	**ΔE (mV)**			
	BzO^-	AcO^-	Cl^-	Br^-
1	-[b]	81	86	25
[**1**.Na^+]	-[b]	83	90	-[b]
2	47	86	70	14
[**2**.Na^+]	-[b]	148	94	-[b]

[a] ΔE is defined as E_{pa} (free receptor) – E_{pa} (complex). [b] Precipitaion occurred.

Although the agreement in the electrochemical and NMR spectroscopic titration suggests that both types of changes originate from receptor-anion binding in the absence and presence of cation, the data in Tables 3.2 and 3.5 reveal that the magnitude of the binding constant does not necessarily correspond to the actual magnitude of anion-induced changes in redox potential. For example, the acetate anion shows the highest magnitude in changes of the redox properties in receptor **2** in the presence of cation, whereas no significant change of redox potential for receptor **2** towards bromide in the presence of cation was observed. However, the binding constant calculated from ^{1}H-NMR titration for bromide anion in the presence of cation are higher than any other anion, including acetate anion. The same behavior was also reported for pyrrole-ferrocene systems [41], [42]. The phenomena that raise this disparity are still not entirely clear.